Microstructure and Phase Stability of INCONEL Alloy 617

W. L. MANKINS, J. C. HOSIER, AND T. H. BASSFORD

INCONEL alloy 617 (54 Ni, 22 Cr, 12.5 Co, 9 Mo, 1 Al, 0.07 C) is a solid-solution alloy with good corrosion resistance and an exceptional combination of high-temperature strength and oxidation resistance. A laboratory study was performed to determine the effects of long-time (215 to over 10,000 h) exposure to temperatures up to 2000°F (1093°C) on the microstructure and phase stability of the alloy. To investigate the strengthening response exhibited by the alloy during high-temperature exposure, microstructures were correlated with mechanical properties. The major phase present in the alloy after exposure to all temperatures from 1200 to 2000°F (649 to 1093°C) was found to be $M_{23}C_6$. The phase precipitated as discrete particles and remained stable at all temperatures. No MC or M_6C carbides were found. A small amount of gamma prime was found in samples exposed at 1200°F (649°C) and 1400°F (760°C). A PHACOMP analysis indicated 0.63 pct gamma prime could form. No topological close-packed phases such as sigma, mu, and chi were found. Strengthening of the alloy during exposure to temperature was found to result primarily from the precipitation of $M_{23}C_6$. The phase provides effective strengthening because it precipitates in discrete particles and remains stable at temperatures to 2000°F (1093°C). The amount of gamma prime formed is not sufficient to cause appreciable hardening, but it does provide some strengthening at 1200 to 1400°F (649 to 760°C).

INCONEL* alloy 617 is a nickel-chromium-cobalt-molybdenum alloy characterized by good cyclic-oxidation resistance at 2000°F (1093°C) and high creep-rupture strength at temperatures from 1200°F (649°C) to 2000°F (1093°C). The alloy is solid-solution-strengthened and is used in the annealed condition.

Alloy 617 exhibits a strengthening response during extended exposure to intermediate temperatures. As shown in Fig. 1, the microstructure of the alloy after such exposure contains copious amounts of precipitate in both grain-boundary and intragranular areas. The work reported here was done to identify the phases present, to determine the stability of the phases, and to investigate the strengthening mechanisms by correlating microstructures with mechanical properties.

*INCONEL is a registered trademark of The International Nickel Company, Inc.

EXPERIMENTAL PROCEDURE

Creep specimens were selected for the study because they would provide a close approximation of material exposed to temperature under load in actual service. The specimens were 0.252 in. (6.35 mm) diam with a 2.25 in. (57.2 mm) gage length. Table I lists temperatures, stresses, and exposure times for the specimens. The maximum amount of plastic strain recorded for any specimen was 9.39 pct, and the creep curves indicated that none of the specimens had begun tertiary creep.

All specimens were from one heat; the chemical composition is given in Table II. The material was produced as 0.750 in. (19 mm) diam hot-rolled rod

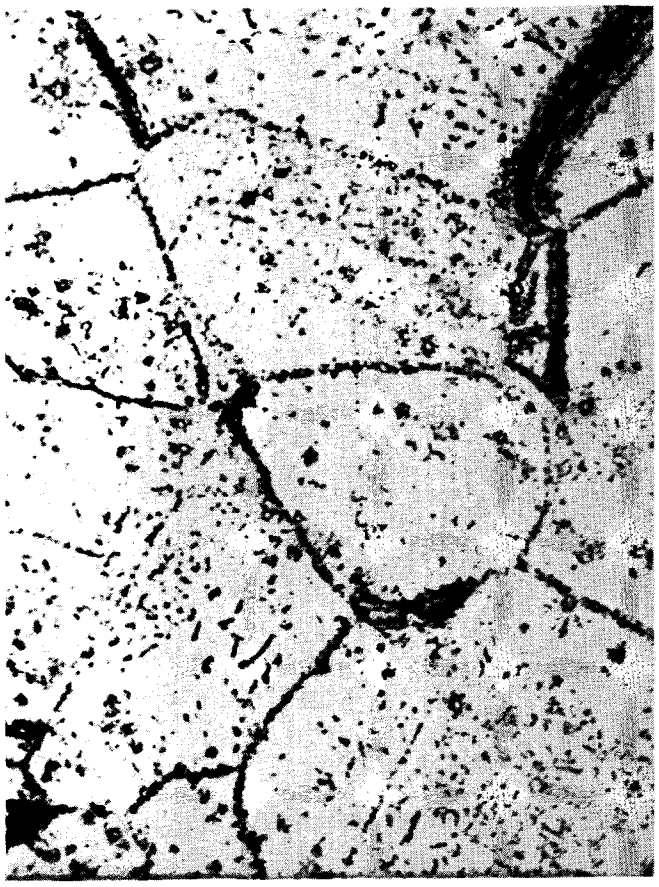

Fig. 1—Microstructure of creep-test specimen subjected to 1400°F (760°C) and 15 ksi (103 MPa) for 10,330.5 h. Magnification 500 times. Specimen No. 2.

W. L. MANKINS, J. C. HOSIER, and T. H. BASSFORD are Metallurgical Project Leaders and Chief Mechanical Testing Engineer, respectively, Huntington Alloy Products Division, The International Nickel Company, Inc., Huntington, W. Va. 25720.

Manuscript submitted October 26, 1973.

Table I. Creep-Test Conditions to Which Samples Were Exposed Prior to Metallographic Study

Specimen No.	Temperature °F	Temperature °C	Stress psi	Stress MPa	Duration,* h
1	1200	649	35,000	241	956.0
2	1400	760	15,000	103	10,330.5
3	1500	816	10,000	69	3,023.0
4	1600	871	4,000	28	666.3
5	1800	982	3,000	21	379.4
6	2000	1093	1,000	7	215.3

*All tests were discontinued before rupture.

Table II. Chemical Composition, Wt Pct, of Material Studied

Chromium	22.51
Cobalt	12.67
Molybdenum	8.91
Aluminum	1.05
Titanium	0.41
Carbon	0.07
Nickel	Remainder

and was given a treatment of 2150°F (1177°C)/1 h, air cool, before being creep-tested.

Samples for optical microscopy were prepared from the gage length of each creep specimen. The samples, about 0.250 in. (6.35 mm) diam, were mounted, polished, and electrolytically etched at 10 V and 0.5 A in 80 pct phosphoric acid/20 pct distilled water. Current density was 10 A/in.^{2} (15.7 mA/mm^2). Etching time was 3 to 7 s.

The electron microscopy was done on an RCA EMU-3G instrument at 100 kV. Parlodion extraction replicas were made using standard carbon-shadowing techniques. Negative replicas were shadowed with chromium and backed by a thin layer of carbon. Thin foils for transmission electron microscopy were produced by electrical discharge machining of discs from the gage lengths of the creep-test specimens. The discs were dimpled by a jet technique with an electrolyte of 10 pct nitric acid/90 pct water. Final electropolishing to perforation was performed with 10 pct perchloric acid/90 pct acetic acid and a platinum cathode.

Precipitated phases were identified by X-ray diffraction, and elemental abundances were determined by X-ray fluorescence. Quantitative extractions were also used to make comparisons. Extractions were done with 10 pct hydrochloric acid plus 1 pct tartaric acid in methanol and also with 1 pct ammonium sulfate plus 1 pct tartaric acid in distilled water. In some cases, the values obtained were reinforced with duplicate extractions.

RESULTS AND DISCUSSION

An overview of the microstructures as they appear at a magnification of 500 times under the light microscope is presented in Fig. 2. The photomicrographs permit description of the precipitates only in general terms since in most cases the precipitates are too fine to be evaluated by optical microscopy. A detailed evaluation, based on the results of electron microscopy, is given later.

Fig. 2(*a*) shows the microstructure of the alloy in the as-annealed condition (the specimen was from a control sample that was not creep-tested). The intragranular areas contain a few widely scattered precipitates. The grain boundaries exhibit some very fine precipitates that are difficult to resolve with the light microscope.

The effects of long-time exposure to high temperatures are shown in Figs. 2(*b*) through 2(*g*). The specimens were from creep-test samples that were exposed as shown in Table I. Four of the specimens (2(*b*) through 2(*f*)) contain particles of TiN and Ti(CN) that were identified optically by their size, angular shape, and characteristic pink, orange or salmon color.

Fig. 2(*b*), the sample exposed at 1200°F (649°C), shows fine, discrete particles in the grain boundaries. The intragranular particles are somewhat larger than those in the as-annealed sample and have more pronounced polyhedral shapes. Some precipitates are also visible on twin lines.

Figs. 2(*c*), 2(*d*), and 2(*e*) show that the amount of precipitation increases in both grain boundaries and intragranular areas with exposure to temperatures of 1400 to 1600°F (760 to 871°C). The microstructures indicate that at those temperatures the nuclei of the precipitates are stable and the rate of nucleation increases. The particles would tend to remain small and discrete because of the relatively slow diffusion rate, at these temperatures, of large elements in the precipitates. At some temperature, perhaps near 1600°F (871°C) for this alloy, the rate of nucleation would reach a maximum because of the opposing tendencies of nucleation and growth.

Fig. 2(*f*) shows that exposure to 1800°F (982°C) results in less precipitation than the amounts present in samples exposed to lower temperatures. The higher exposure temperature does not favor nucleation. As indicated by particle size, growth rate is not rapid either.

Fig. 2(*g*), 2000°F (1093°C) exposure, shows few intragranular particles, but the particle size is somewhat larger. This temperature favors growth of the particles since diffusion can occur more readily than at lower temperatures.

Identification of Carbides and Carbonitrides

Analysis of Debye-Scherrer X-ray patterns for a complex alloy is complicated because the lines obtained are frequently common to more than one phase. Table III shows the phases identified and their relative amounts.

As shown in Table III, $M_{23}C_6$ (where M is Cr + Mo) is the predominant phase at all exposure temperatures

Table III. Identification of Extracted Phases

Phase	Temperature Range °F	Temperature Range °C	Amount
$M_{23}C_6$	1200-2000	649-1093	Very abundant
$Cr_{23}C_6$	1200-2000	649-1093	Rare
TiN	1200-2000	649-1093	Rare
CrMo (C, N)	1200-2000	649-1093	Very rare
γ' (Ni_3Al)	1200-1400	649-760	Rare

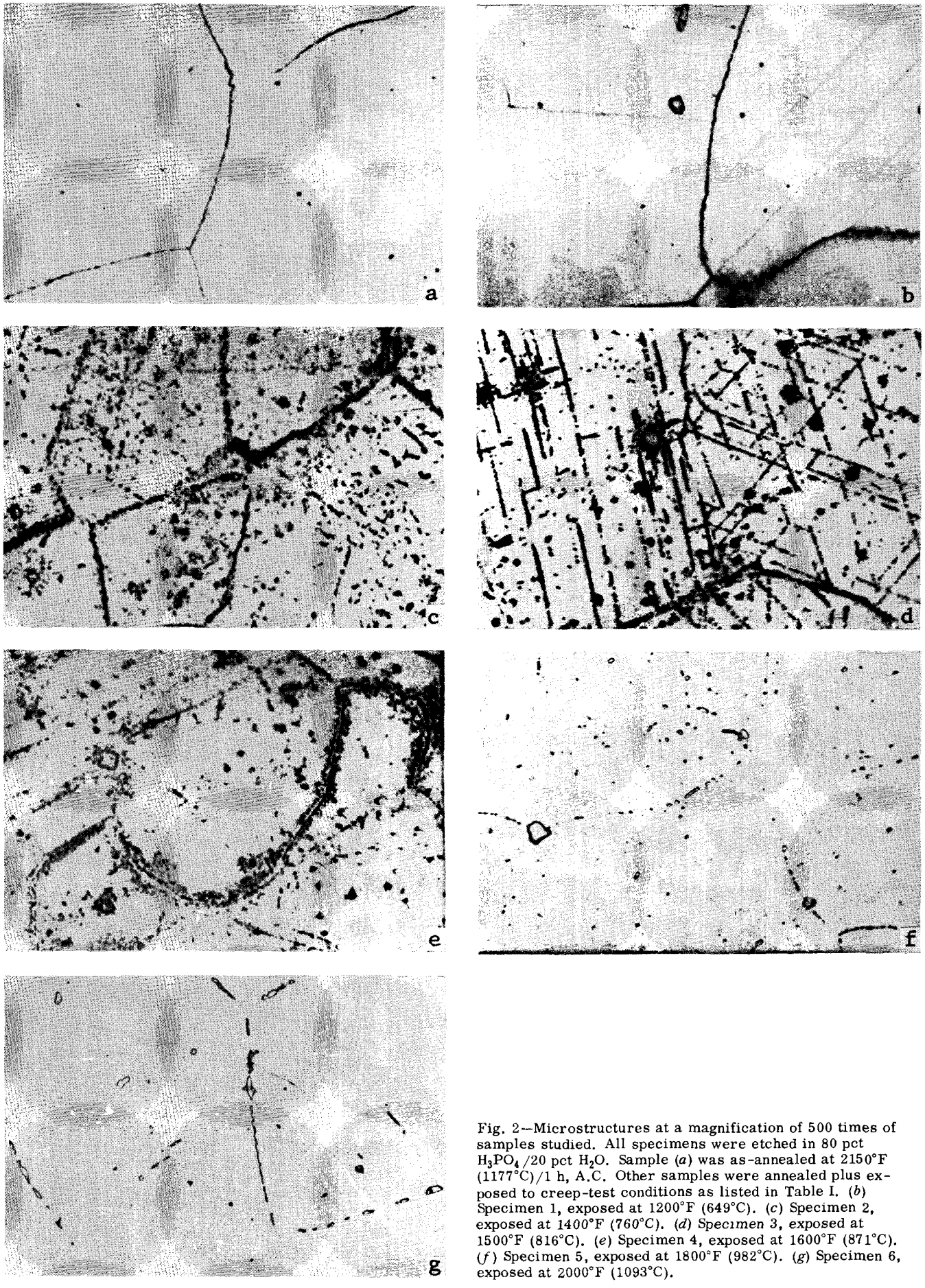

Fig. 2—Microstructures at a magnification of 500 times of samples studied. All specimens were etched in 80 pct H_3PO_4/20 pct H_2O. Sample (*a*) was as-annealed at 2150°F (1177°C)/1 h, A.C. Other samples were annealed plus exposed to creep-test conditions as listed in Table I. (*b*) Specimen 1, exposed at 1200°F (649°C). (*c*) Specimen 2, exposed at 1400°F (760°C). (*d*) Specimen 3, exposed at 1500°F (816°C). (*e*) Specimen 4, exposed at 1600°F (871°C). (*f*) Specimen 5, exposed at 1800°F (982°C). (*g*) Specimen 6, exposed at 2000°F (1093°C).

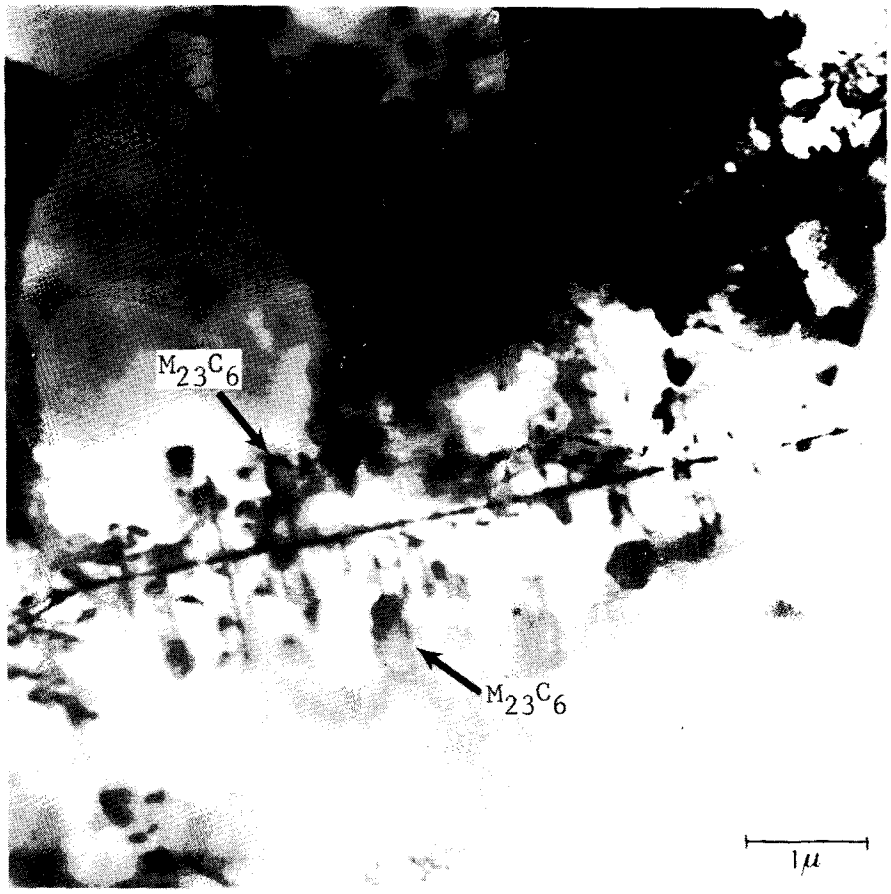

Fig. 3—Microstructure of specimen exposed to 1400°F (760°C) and 15 ksi (103 MPa) for 10,330.5 h. Thin foil. Magnification 16,000 times. Specimen No. 2.

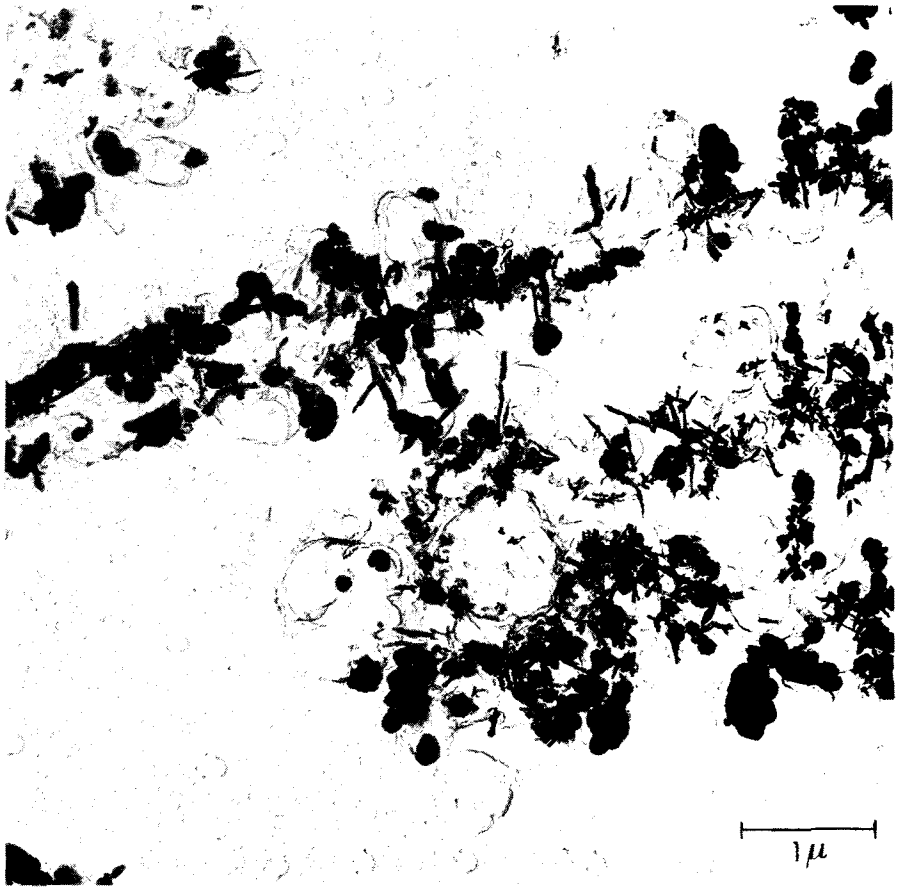

Fig. 4—Extraction replica of grain-boundary precipitate shown in Fig. 3. Magnification 17,500 times. Specimen No. 2.

from 1200°F (649°C) to 2000°F (1093°C). The $Cr_{23}C_6$ phase also was identified from the experimental lines, but the abundance calculations showed a high concentration of molybdenum, indicating that the $Cr_{23}C_6$ phase was rare.

The electron micrograph in Fig. 3 shows typical grain-boundary particles that were identified by selected-area diffraction. To provide a better indication of the amount of carbide present, the extraction replica shown in Fig. 4 was prepared. It depicts the precipitate clearer than the thin foil. Both micrographs are at the same magnification and show comparable precipitates. The selected-area diffraction pattern from the replica and the electron-diffraction results from the thin foil (see Fig. 12) conclusively demonstrated that the carbide was $M_{23}C_6$.

In addition to the TiN and Ti(C, N) particles that were observed with light microscopy, a CrMo(C, N) phase was identified in all specimens by X-ray diffraction of the extracted residues. The phase was not identified by electron diffraction, indicating that it was very rare.

Some of the precipitated carbides displayed an interesting morphology. In some cases, the intragranular carbides precipitated around polyhedral particles in sunburst patterns as illustrated in Fig. 5. The center particles were visible under the light microscope, but they did not have sufficient size or coloration to suggest that they were precipitates of the TiN type. Neither did they have the triangular shape usually associated with MC precipitates.

Much effort was expended in attempts to obtain an electron-diffraction pattern for the center particles, but little success was achieved. The particles were too thick to obtain an electron-diffraction pattern from an extraction replica, and thin foils could not retain the particles. When a particle in a foil was thinned to the point that it might have been penetrated by the beam, the surrounding area would be dissolved, and the particle would drop through the hole. Fig. 6, in which the polyhedral shaped particle is missing from the carbide cluster, shows one of the thin-foil attempts.

Selected-area diffraction and electron diffraction did not provide an identification of the polyhedral particles. The work of Kegg and Silcock,[1] however, showed the shapes of isolated intragranular particles of $M_{23}C_6$ to be very similar to the shapes of the particles shown here at the centers of the carbide clusters.

The phase was found to exist throughout the temperature range studied. Fig. 7 distinctly shows the polyhedral particles in samples exposed at 1800°F (982°C). As shown in the photomicrograph, most of the fine, irregular precipitate that surrounded the particles at lower temperatures is in solution at 1800°F (982°C). The X-ray diffraction data showed that $M_{23}C_6$ was present at all temperatures studied to 2000°F (1093°C). It was therefore concluded that the polyhedral particles were $M_{23}C_6$ carbides.

Lewis and Hattersley[2] suggested that the majority of intragranular precipitation nucleates on dislocations that are generated by the growth of existing particles. The present authors propose that the 2150°F (1177°C) anneal is not sufficient to solution all of the carbides present and that the carbides grow as the alloy is cooled from the annealing temperature. The carbide growth would create dislocations on which the smaller carbides could precipitate during subsequent exposure to temperature and produce the observed sunburst patterns. This proposal is supported by Figs. 2(*a*) and 2(*b*), in which the only intragranular carbides visible are solitary particles. Both of those specimens were examined by transmission electron microscopy. As shown in Fig. 8, the only intragranular carbides present were the polyhedral particles.

Extensive carbide precipitation occurred along twin boundaries. This is evident in the optical photomicrographs shown in Figs. 2(*c*) through 2(*e*) and in the extraction replica shown in Fig. 9.

The thin foils examined in this study showed the grain-boundary precipitate to be discontinuous. Fig. 10 illustrates a grain boundary marked by discrete precipitate that was identified as $M_{23}C_6$. The matrix area exhibits an abundance of $M_{23}C_6$ which also is discrete. The discrete nature of the grain-boundary carbides enhances mechanical properties because it causes pinning of the boundary and decreases grain-boundary sliding. Betteridge[3] observed the same effect in a similar alloy system and also found that $M_{23}C_6$ must precipitate at the grain boundaries as well as within the matrix or creep-rupture properties would be poor (short life and low elongation).

The MC and M_6C carbides were not found in any of the samples. They may have been present as minor trace phases, but sufficient diffraction lines for conclusive identification were not obtained.

Topological close-packed phases such as sigma, mu, and chi were not found in any sample.

Collins[4] has shown that some commonly made assumptions concerning precipitation of carbides in nickel-base superalloys are not always correct. Two assumptions found invalid by Collins were also found to be invalid in this study. They are 1) that if the MO + W is greater than 6 wt pct, the M_6C carbide will form in lieu of $M_{23}C_6$ and 2) that half of the carbon present will form MC and half will form either M_6C or $M_{23}C_6$. The mechanism by which $M_{23}C_6$ precipitates as the major or sole carbide in alloy 617 has not been fully determined and is the subject of further research.

Identification of Gamma Prime

INCONEL alloy 617 was designed to be a solid-solution-hardened alloy with age-hardening constituents held to low values. Aluminum was added at a nominal 1.0 wt pct level to provide required oxidation resistance. Experience suggested that this amount of aluminum and 0.35 wt pct titanium would not promote significant precipitation hardening. Early development work on the alloy did not disclose the presence of the gamma prime phase. The initial work in this study, however, showed that a small amount of gamma prime (fcc Ni_3Al) was precipitated after exposure at 1400°F (760°C) for more than 10,000 h.

A modified PHACOMP analysis performed on the composition predicted that only 0.63 pct gamma prime would form. The predicted lattice parameters (a_0) were 3.55052 for the gamma prime and 3.5554 for the residual matrix, with only 0.1413 pct mismatch.

The gamma prime phase was first observed in a thin foil. It was decorated by dislocations as shown in Fig. 11. The amount of gamma prime present was scant as predicted by PHACOMP analysis. The dislocations

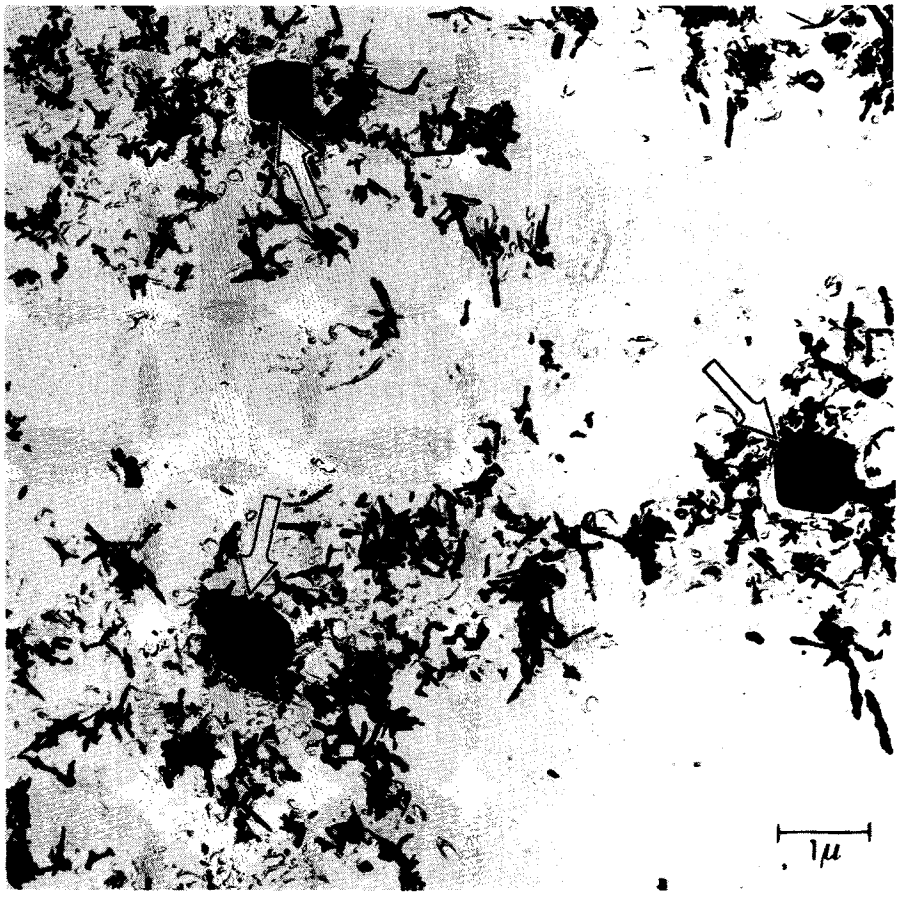

Fig. 5—Extraction replica of Specimen No. 3 showing intragranular carbides precipitated around polyhedral particles. Specimen was exposed to 1500°F (816°C) and 10 ksi (69 MPa) for 3,023 h. Magnification about 12,000 times.

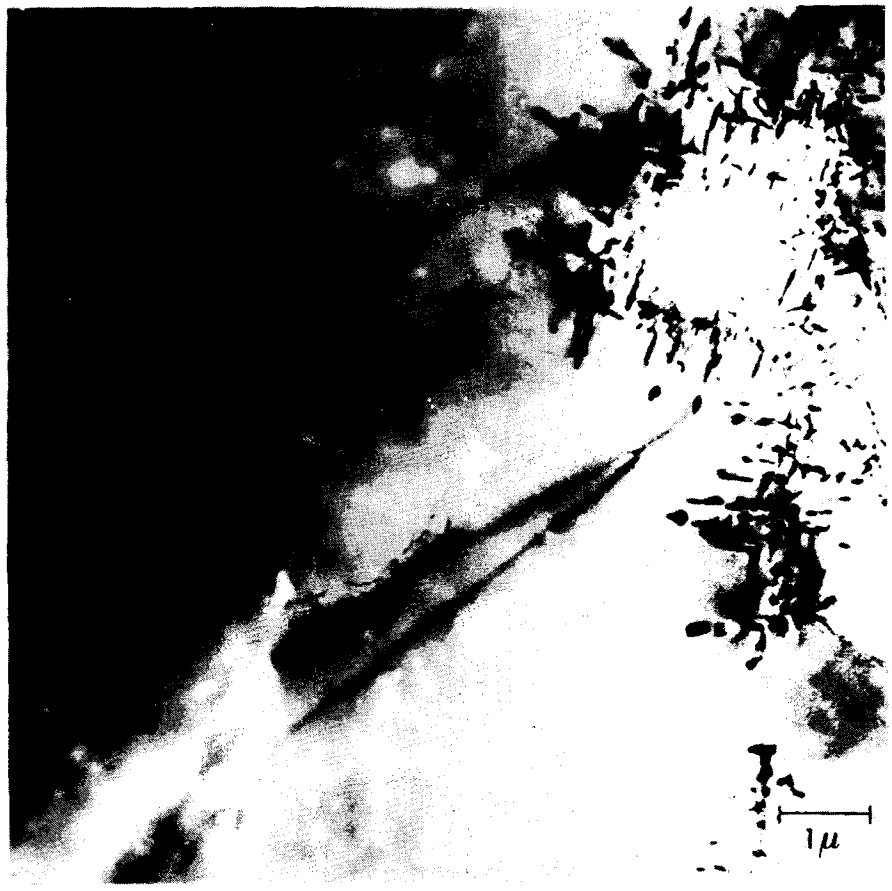

Fig. 6—Thin foil of Specimen No. 3 showing carbide cluster without center particle. Specimen was exposed to 1500°F (816°C) and 10 ksi (69 MPa) for 3,023 h. Magnification about 12,000 times.

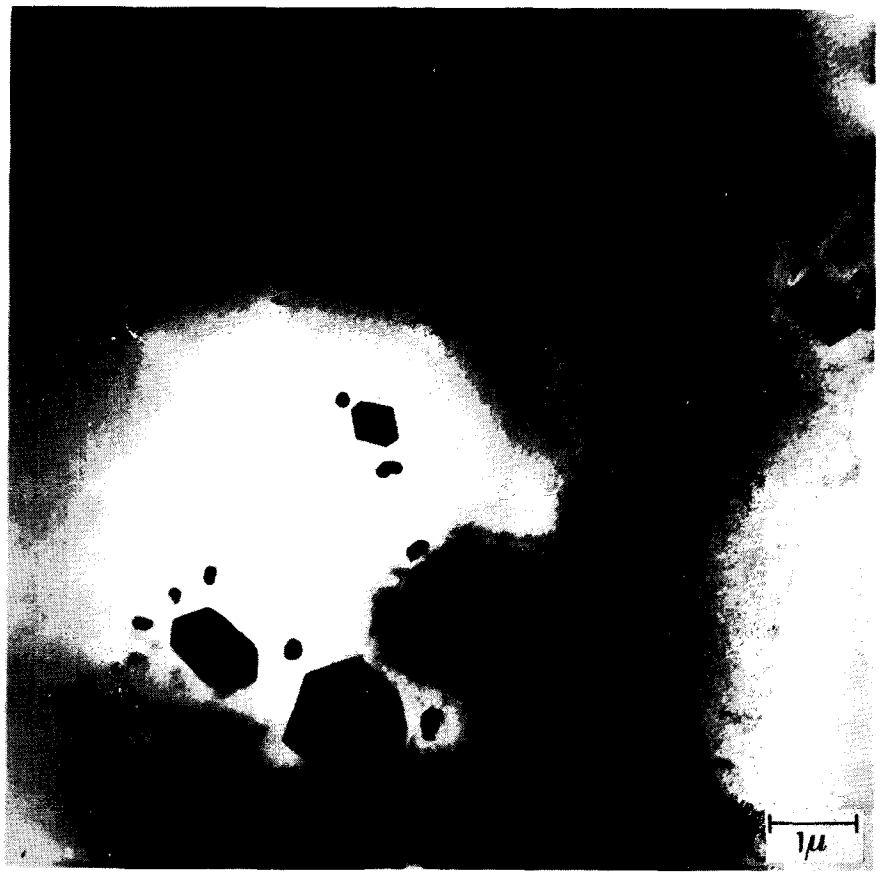

Fig. 7—Polyhedral particles in Specimen No. 5. Exposure was 1800°F (982°C) and 3.0 ksi (21 MPa) for 379.4 h. Magnification about 11,500 times.

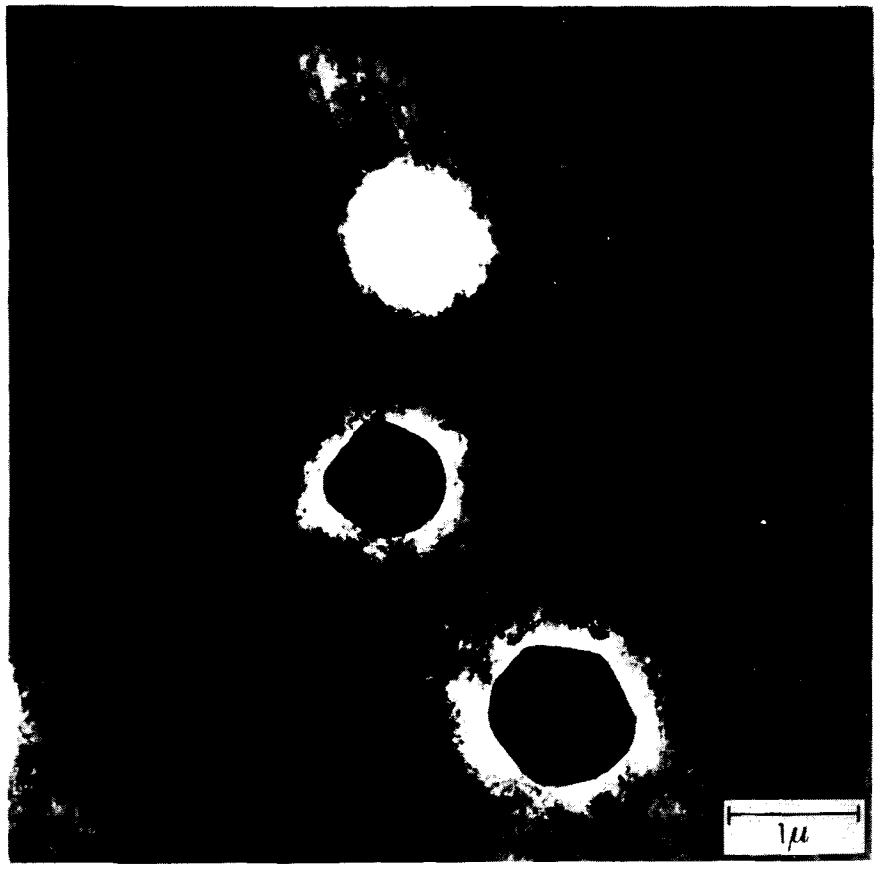

Fig. 8—Polyhedral particles in Specimen No. 1. Exposure was 1200°F (649°C) and 35,000 psi (241 MPa) for 956 h. Magnification 17,000 times.

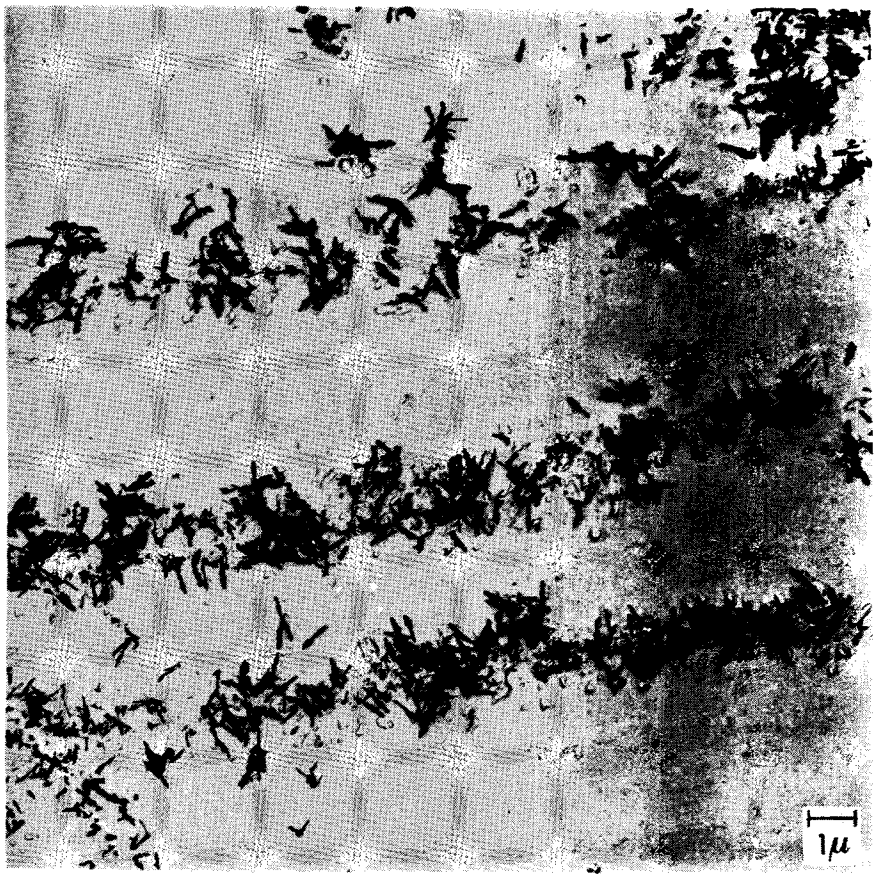

Fig. 9—Extraction replica of carbide precipitation along twin boundaries in specimen exposed to 1500°F (816°C) and 10 ksi (69 MPa) for 3,023 h. Magnification about 6,000 times. Specimen No. 3.

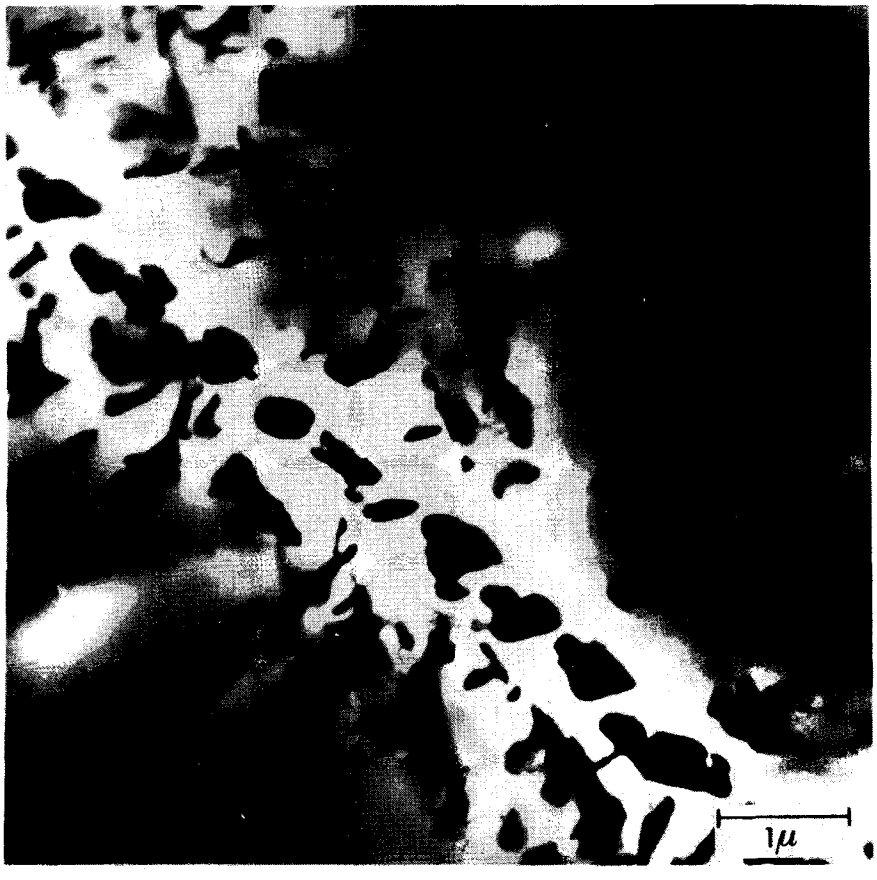

Fig. 10—Discrete precipitate in grain boundary of specimen exposed to 1600°F (871°C) and 4.0 ksi (28 MPa) for 666.3 h. Magnification 17,000 times. Specimen No. 4.

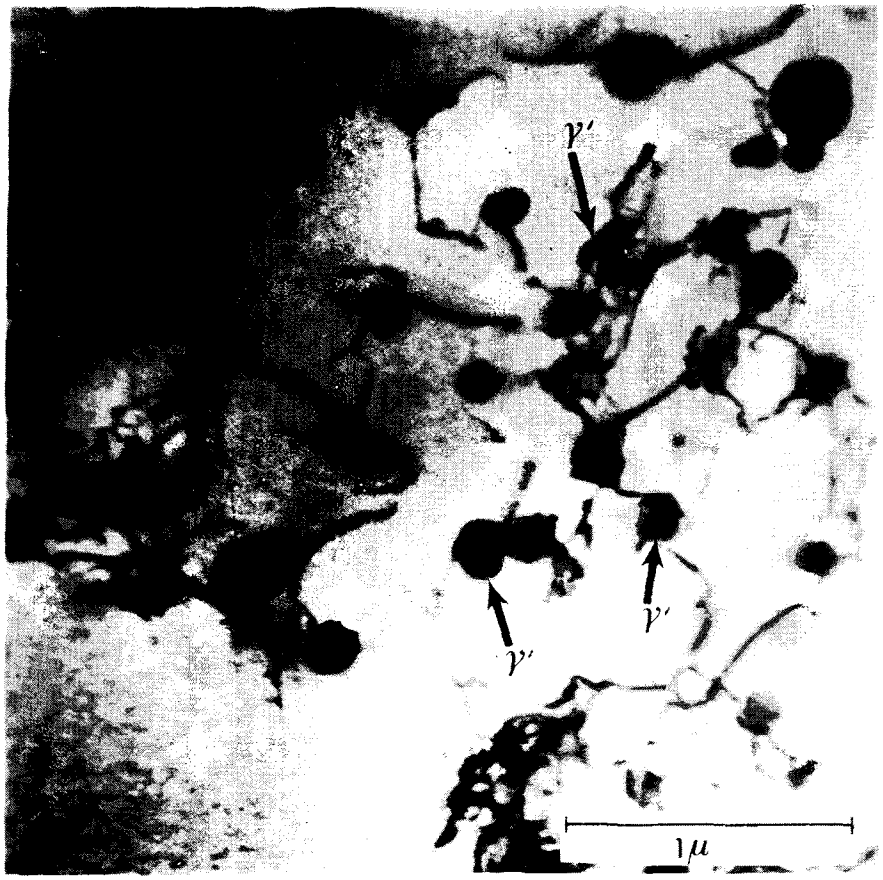

Fig. 11—Thin foil showing gamma prime phase in specimen exposed to 1400°F (760°C) and 15 ksi (103 MPa) for 10,330.5 h. Magnification about 38,000 times. Specimen No. 2.

were evenly distributed in well-defined coarse cells. The gamma prime and dislocations interact, resulting in interfacial networks.

Electron-diffraction patterns of Specimens 1 and 2, which were exposed at 1200°F (649°C) and 1400°F (760°C), respectively, showed the superlattice spots for the gamma prime and made the identification positive. Fig. 12, the diffraction pattern for Specimen 1, shows matrix, carbide, and gamma prime superlattice spots. The zone axis is [211] and with the (hkl) values shown becomes [1$\bar{1}$2]. The superlattice spots may be somewhat difficult to discern but five spots are present as indicated by arrows. The schematic reproduction shows the spot pattern with greater clarity. The gamma matrix was indexed with a_0 = 3.55Å; the gamma prime with a_0 = 3.53Å, and the carbide phase with a_0 = 10.80Å. The percent mismatch from the experimental data is 0.595 pct; 0.1413 pct was predicted by PHACOMP.

Table III shows the presence of gamma prime in X-ray patterns from extracted residues. The abundances indicate the presence of gamma prime at 1200°F (649°C) and 1400°F (760°C) as noted by the increased concentration of nickel in the residue. This result supports the earlier finding in that no superlattice spots were found for samples that had been subjected to temperatures in excess of 1400°F (760°C). Since gamma prime was found at 1400°F (760°C) but not at 1500°F (816°C), the gamma prime solvus is between those temperatures.

The existence of gamma prime in the alloy is thought to be influenced by the molybdenum that is present. Loomis[5] showed that Mo reduced the solubility for aluminum in the gamma matrix of a Ni-Cr-Al-Mo alloy and significantly increased the weight fraction of gamma prime. Molybdenum is known to prevent overaging of the gamma prime phase and thus its contribution is dual: solid-solution hardness and gamma prime catalyst.

The presence of molybdenum and cobalt in combination apparently produces a synergistic interaction; the combined strengthening effect is greater than the sum of the effects of the elements individually. The effect has also been observed[6,7,8] in other alloy systems.

Mechanical Properties

After short-time (50-h) exposure to 1200°F (649°C) and 1400°F (760°C), the amount of gamma prime formed is small, and it has been shown[9] that its effect on mechanical properties is slight. However, 1000-h exposures at temperatures from 1200 to 1600°F (649 to 871°C) cause significant improvements in room-temperature tensile properties. Table IV shows the tensile values obtained. The room-temperature yield strength improves 56 and 63 pct after 1200°F (649°C) and 1300°F (704°C) exposure, respectively, while the room-temperature tensile strength increases by 26 pct for both test conditions. The tensile properties decrease only slightly in the 1400°F to 1600°F (760 to 871°C) temperature span. The properties are aided by the $M_{23}C_6$ carbide precipitation previously discussed.

Samples that had been given the 50- and 1000-h exposures to temperatures of 1200 to 1600°F (649 to 871°C) were also impact tested to demonstrate the metallurgical stability of the alloy. The Charpy V-notch results shown in Fig. 13 indicate an impact strength of over 240 ft-lb (325 J) prior to exposure

Table IV. Effect of Exposure to Intermediate Temperatures on Room-Temperature Mechanical Properties

Exposure* Temperature °F	°C	Exposure Time, h	Yield Strength (0.2 pct Offset) ksi	MPa	Tensile Strength ksi	MPa	Elongation, pct	Reduction of Area, pct	Hardness, *Rb*
No exposure		–	42.9	298	106.6	735	70.0	57.2	81
1200	649	50	50.0	345	115.0	793	63.0	59.9	82
		1000	66.5	458	135.0	931	37.1	29.8	94
1300	704	50	62.9	434	125.9	868	51.0	43.2	93
		1000	70.0	483	135.0	931	36.7	18.8	94
1400	760	50	50.5	348	116.2	801	44.0	36.9	89
		1000	52.0	358	124.5	858	41.4	39.5	88
1500	816	50	48.9	337	115.9	799	43.0	40.6	90
		1000	49.5	341	119.5	824	43.5	36.2	87
1600	871	50	47.4	327	115.6	797	47.0	37.2	87
		1000	47.5	328	118.5	817	46.4	43.2	84

*All specimens were given a solution-treatment of 2150°F (1177°C)/1 h, A.C., before exposure.

and over 190 ft-lb (258 J) after 50 h at 1200°F (649°C). The minimum value obtained was about 50 ft-lb (68 J) after 1000 h of exposure to 1200°F (649°C). The 1000-h samples show only a slight increase in impact strength between 1200°F (649°C) and 1400°F (760°C), the temperature range where gamma prime would be influencing the results. The 50-h samples show a sharp decrease in impact strength over the same temperature range.

From 1400 to 1600°F (760 to 871°C), the impact strength is improved, and this is to be expected in view of the microstructures that have been presented. That is the temperature range in which the numerous $M_{23}C_6$ carbides precipitate. Because they are discrete particles they provide strengthening and tend to reduce embrittling effects related to a film morphology.

INCONEL alloy 617 is used for its exceptional creep and rupture properties at temperatures in excess of 1800°F (982°C). Fig. 14 compares rupture properties of this alloy with those of INCONEL alloy 625. Unlike INCONEL alloy 625, which depends on a sluggish precipitation of Ni- and Cb-rich gamma prime for its strengthening, INCONEL alloy 617 achieves its strengthening through the precipitation of stable, discrete $M_{23}C_6$ carbides. It therefore maintains its strength in the temperature range (1400 to 1800°F) (760 to 982°C) where gamma prime is in solution. It can be seen in Fig. 14

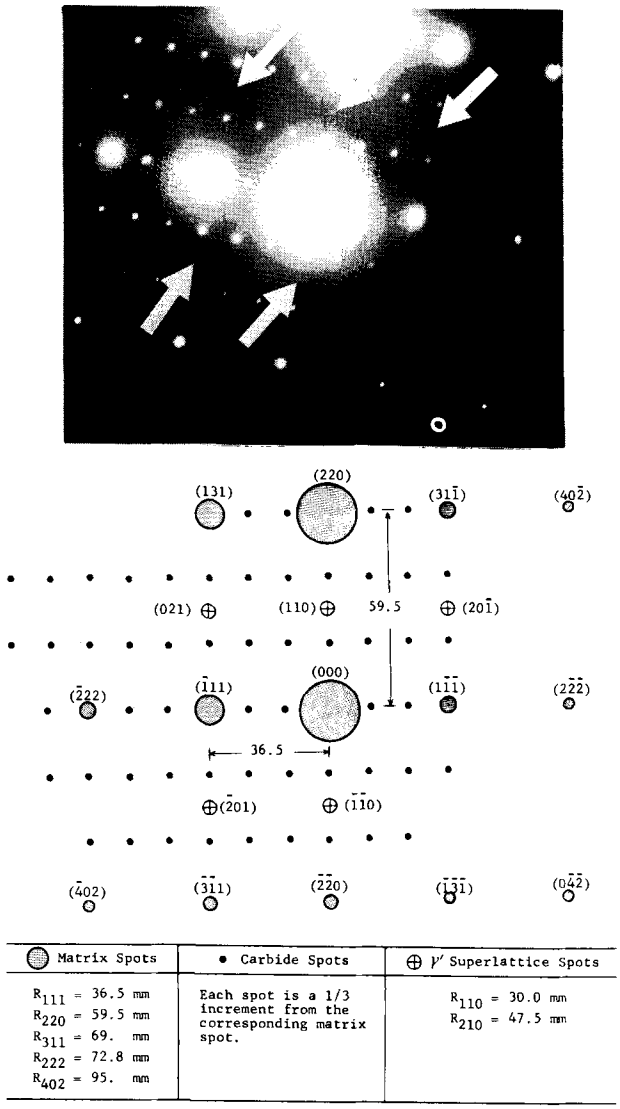

Fig. 12—Electron diffraction pattern of thin foil from Specimen 1. Specimen exposure was 1200°F (649°C) and 35 ksi (241 MPa) for 956 h. The faint gamma prime superlattice spots are indicated by arrows. Zone axis is [1$\bar{1}$2].

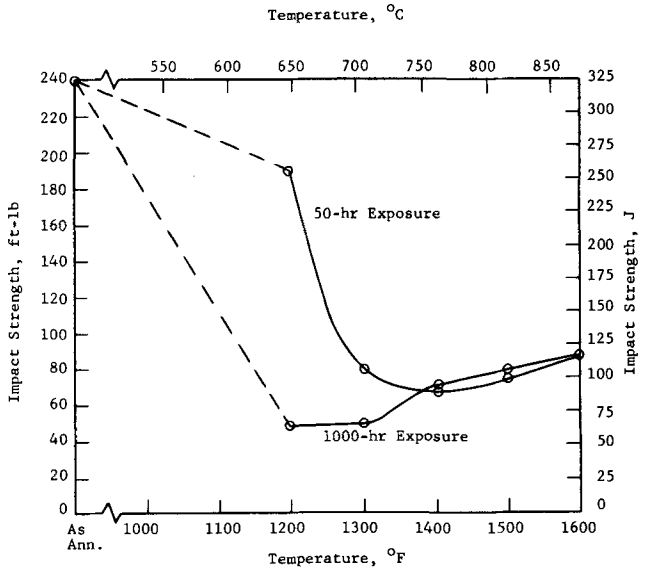

Fig. 13—Metallurgical stability of alloy 617 as indicated by room-temperature impact strength (Charpy V-notch) after exposure to intermediate temperatures.

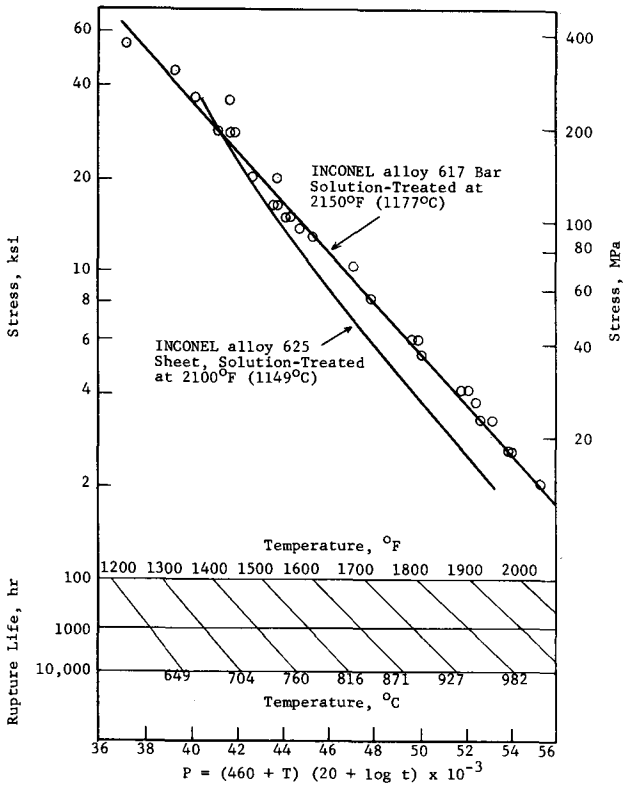

Fig. 14—Larson-Miller parameter plot of rupture strengths of INCONEL alloys 617 and 625. In the parameter, T is temperature in °F and t is time in h.

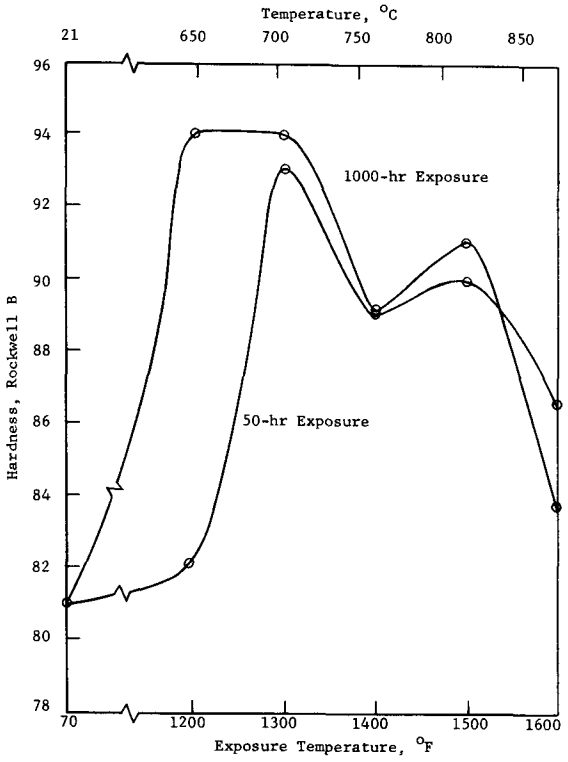

Fig. 15—Effect of high-temperature exposure on the room-temperature hardness of INCONEL alloy 617. Specimens were from 0.750-in. (19-mm) diam hot-rolled rod solution treated at 2150°F (1177°C)/2 h, A.C.

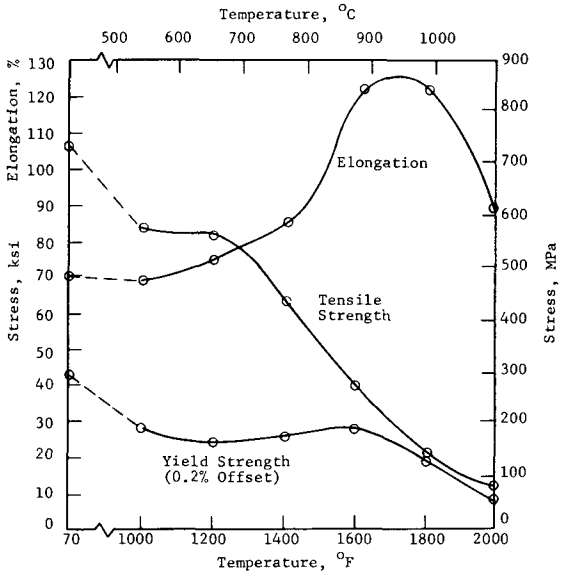

Fig. 16—Effect of temperature on tensile properties of INCONEL alloy 617. Specimens were from 0.750-in. (19-mm) diam hot-rolled rod solution treated at 2150°F (1177°C)/2 h, A.C.

that INCONEL alloy 625 has better rupture properties at temperatures less than 1400°F (760°C). The curves intersect at about 1400°F, and the higher temperatures favor INCONEL alloy 617.

The age-hardening response of alloy 617 can be demonstrated with the hardness data shown in Fig. 15. The material had a hardness of 81 R_b in the annealed condition, and 50 h at 1200°F (649°C) increased the hardness by only one point. When the time was extended to 1000 h, however, the hardness increased to 94 R_b. The hardness level remains the same at 1300°F (704°C) and then decreases as gamma prime solutioning begins. At higher temperatures, the hardness recovers because of extensive carbide precipitation as shown in the microstructures. As indicated by these results, the amount of gamma prime precipitated is not sufficient to cause appreciable hardening.

Short-time high-temperature tensile data show that alloy 617 maintains a high level of strength to 2000°F (1093°C). Fig. 16 gives values for annealed hot-rolled rod. The yield strength is nearly constant at temperatures from 1000°F (538°C) to 1700°F (927°C). This results from the combined effects of solid-solution hardening and the precipitation of discrete particles of stable $M_{23}C_6$.

SUMMARY

The microstructure of INCONEL alloy 617 was studied after long-time exposure to temperatures of 1200°F (649°C) to 2000°F (1093°C). The major phase present in the alloy after such exposure was found to be $M_{23}C_6$. A small amount of gamma prime was found in samples exposed at 1200°F (649°C) and 1400°F (760°C). The CrMo(C, N) phase was identified in all specimens, but the phase was determined to be very rare. No MC or M_6C was conclusively identified in any sample. Also not found were topological close-packed phases such as sigma, mu, and chi.

The alloy precipitates polyhedral particles of stable $M_{23}C_6$ carbides intragranularly during cooling from the

annealing temperature. During subsequent exposure to temperatures over 1400°F (760°C), the alloy precipitates additional discrete $M_{23}C_6$ carbides in the grain boundaries, along twin boundaries, and around the polyhedral particles. Only $M_{23}C_6$ carbides form and they always form as discrete particles. The precise metallurgical reasons for carbide precipitation of that nature are not fully understood, but the phenomenon is thought to be related to the synergistic interaction of molybdenum and cobalt.

The gamma prime phase in the alloy is not prone to overaging or transformation. A sample exposed to 1400°F (760°C) for over 10,000 h exhibited gamma prime of the stable Ni_3Al type, indicating that the gamma prime does not transform to any morphologically deleterious phase after long exposure times. Overaging of the gamma prime is though to be retarded by the combined presence of molybdenum and cobalt.

The microstructures correlate with the alloy's mechanical properties. Although the amount of gamma prime formed is not sufficient to cause appreciable hardening, it does provide some strengthening at temperatures of 1200 to 1400°F (649 to 760°C). At higher temperatures, which solution the gamma prime, the alloy is strengthened by the precipitation of stable, discrete $M_{23}C_6$ carbides.

ACKNOWLEDGMENT

The authors wish to acknowledge the contributions of R. D. Barrett, who prepared the electron-microscopy specimens, and H. C. Erwin, who prepared the photomicrographs.

REFERENCES

1. C. R. Kegg and J. M. Silcock: *Scr. Met.*, 1972, vol. 6, pp. 1083-86.
2. M. H. Lewis and B. Hattersley: *Acta Met.*, 1965, vol. 13, pp. 1159-68.
3. W. Betteridge: *The Nimonic Alloys*, pp. 66-117, Edward Arnold Ltd., London, 1959.
4. H. E. Collins: *ASM Trans.*, 1969, vol. 62, pp. 82-104.
5. W. T. Loomis, J. W. Freeman, and D. L. Sponseller: *Met. Trans.*, 1972, vol. 3, pp. 989-98.
6. S. Floreen and G. R. Speich: *ASM Trans.*, 1964, vol. 67, pp. 714-26.
7. R. D. Jones and S. Kapoor: *J. Iron Steel Inst.*, 1973, vol. 211, pp. 226-28.
8. D. T. Peters: *Trans. TMS-AIME*, 1967, vol. 239, p. 1981.
9. J. C. Hosier and D. J. Tillack: *Met. Eng. Quart.*, 1972, vol. 12, pp. 51-55.